NASA TECHNICAL MEMORANDUM

NASA TM X-1625

NASA TM X-1625

HIGH TEMPERATURE CREEP-RUPTURE PROPERTIES OF A TUNGSTEN-URANIUM DIOXIDE CERMET PRODUCED FROM COATED PARTICLES

by Robert J. Buzzard

Lewis Research Center
Cleveland, Ohio

NATIONAL AERONAUTICS AND SPACE ADMINISTRATION • WASHINGTON, D. C. • AUGUST 1968

NASA TM X-1625

HIGH TEMPERATURE CREEP-RUPTURE PROPERTIES OF A TUNGSTEN-URANIUM DIOXIDE CERMET PRODUCED FROM COATED PARTICLES

By Robert J. Buzzard

Lewis Research Center
Cleveland, Ohio

NATIONAL AERONAUTICS AND SPACE ADMINISTRATION

For sale by the Clearinghouse for Federal Scientific and Technical Information
Springfield, Virginia 22151 – CFSTI price $3.00

ABSTRACT

Tungsten-50 volume percent uranium dioxide cermets, produced by roll compaction of tungsten-coated uranium dioxide particles and clad with tungsten, were creep-rupture tested at temperatures of 1080° to 1800° C (1975° to 3272° F) and stresses of 1740 to 14 500 psi (12 to 100 MN/m^2). Rupture life values ranged from 1 to 696 hrs. Additional rupture life values were predicted by use of the Manson-Haferd time-temperature parameter. Isotherms for 0.5 and 1.0 percent creep, and the end of second stage creep, also were constructed by use of this parameter. An attempt was made to describe the role of the UO_2 in the cermet's creep-rupture process.

STAR Category 17

HIGH TEMPERATURE CREEP-RUPTURE PROPERTIES OF A TUNGSTEN-URANIUM DIOXIDE CERMET PRODUCED FROM COATED PARTICLES

by Robert J. Buzzard

Lewis Research Center

SUMMARY

The creep rupture properties of a tungsten clad, tungsten-50 volume percent uranium dioxide (W-50 v/o UO_2) cermet made by roll compaction of tungsten coated uranium dioxide particles were determined at 1080° to 1800° C (1975° to 3272° F). Typical rupture lives ranged from 1 hour at 1450° C (2640° F) to 618 hours at 1080° C (1975° F) for a stress level of 14 500 psi (100 MN/m^2). At a stress level of 5075 psi (35 MN/m^2), typical rupture lives were 4 hours at 1800° C (3272° F) and 158 hours at 1427° C (2600° F). The Manson-Haferd time-temperature parameter was used to predict longer time creep properties of this cermet.

The stress rupture life and ductility of this cermet appear to be controlled by the continuous, vapor deposited tungsten phase. The dispersed UO_2 particles do not appear either to contribute to high temperature strength or to significantly embrittle the cermet. The W-50 v/o UO_2 cermet enters the third stage of creep at relatively low total strain levels (less than 1 percent). For this reason, design calculations for this type of material should be based on creep strain values of 0.5 percent or less.

INTRODUCTION

Cermets composed of mixtures of metal and ceramic phases have been produced for many years by conventional powder metallurgy techniques. One such cermet, consisting of a dispersion of uranium dioxide (UO_2) in a tungsten (W) matrix, is being considered for use in nuclear reactor fuel elements of advanced space power generation systems.

In producing these cermets by blending, compacting, and sintering W and UO_2 powders, nonuniform dispersions can result. As the UO_2 (fuel) loading is increased, the probability of maintaining a completely uniform dispersion decreases; consequently, agglomerates of UO_2 are frequently formed even in the most carefully blended powder metallurgy W-UO_2 cermets. These agglomerates are undesirable from the standpoint of mechanical, physical, and nuclear property considerations. A more promising method of obtaining a uniform dispersion of UO_2 in W at any given fuel loading involves the use of tungsten-coated uranium dioxide particles. During consolidation of these particles, the W particle coating assumes the role of the matrix material, with the UO_2 as the dispersed phase. The use of such coated particles results in a continuously interconnected W matrix and prevents contact of the UO_2 particles at even the highest fuel loadings. Such complete separation of the second phase particles should result in improved properties of the material (refs. 1 and 2).

Since the creep-rupture properties of W-UO_2 cermets produced from coated particles have not been previously characterized, the purpose of this study was to evaluate the creep-rupture properties of this type of cermet in the temperature range of interest for space reactor systems. Sheet specimens containing W-50 volume percent UO_2 (W-50 v/o UO_2) cermet cores were used in this study. The cores were produced by hot roll compaction of tungsten-coated UO_2 particles. After machining to the desired specimen shape, they were completely clad on all surfaces with vapor deposited tungsten. The creep-rupture tests were conducted at temperatures in the range of 1080° to 1800° C (1975° to 3272° F) and stresses of 1740 to 14 500 psi (12 to 100 MN/m^2). The resultant rupture life values ranged from 1 to 696 hours.

The results of these tests are presented in this report as creep curves and as creep and rupture life isotherms obtained by use of the Manson-Haferd linear parameter (ref. 3). The mode of deformation of the cermet is discussed, and the cermet's strength is compared to that of unfueled tungsten.

EXPERIMENTAL METHODS

Test Material

The starting material used in this study was purchased in the form of tungsten-coated uranium-dioxide (UO_2) microspheres. The UO_2 particles were nominally 50 microns in diameter onto which a vapor deposited tungsten coating of 6 to 7 microns thickness was applied by hydrogen reduction of tungsten hexachloride (WCl_6) in a fluidized bed. This coating resulted in a tungsten-to-UO_2 volume ratio of 1 : 1 (W-50 v/o UO_2). The coated particles were formed into fully dense cermet plates by the hot roll compaction process described by Watson, Caves, and Saunders (ref. 2).

Test specimens were prepared by electrical discharge machining the cermet plates into the shape shown in figure 1. After roughening the specimen surfaces with number 180 grit paper to ensure proper bonding of the cladding, the specimens were vibratory

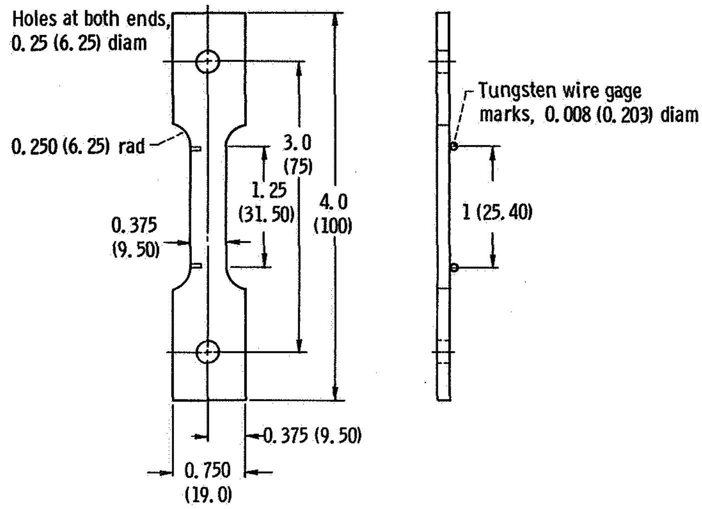

Figure 1. - High-temperature creep-rupture sheet specimen. (Dimensions are in inches (MM).

cleaned in separate water, acetone, and alcohol baths and then purged in hydrogen at about 1350° C for 1 hour. The specimens were then clad on all surfaces by vapor deposition of tungsten.

Chemical analysis of a typical finished W-UO_2 roll-compacted plate with tungsten cladding is presented in table I. The potentially detrimental impurities carbon, fluorine, and chlorine were all controlled to low levels. The microstructure of a finished specimen is shown in figure 2. Note that all of the UO_2 particles are separated by the tungsten

TABLE I. - CHEMICAL ANALYSIS OF TUNGSTEN-50-VOLUME-PERCENT URANIUM DIOXIDE CERMETS WITH TUNGSTEN CLADDING

Element	Concentration
Tungsten (including cladding)	[a]75.2 wt. % (63 vol. %)
Uranium dioxide	[a]24.8 wt. % (37 vol. %)
Carbon	4 ppm
Fluorine	ND[b]
Chlorine	ND[b]

[a]Corresponds to a W-50 vol. % UO_2 core with tungsten cladding.

[b]Not detected (lower limit of detection, 5 ppm).

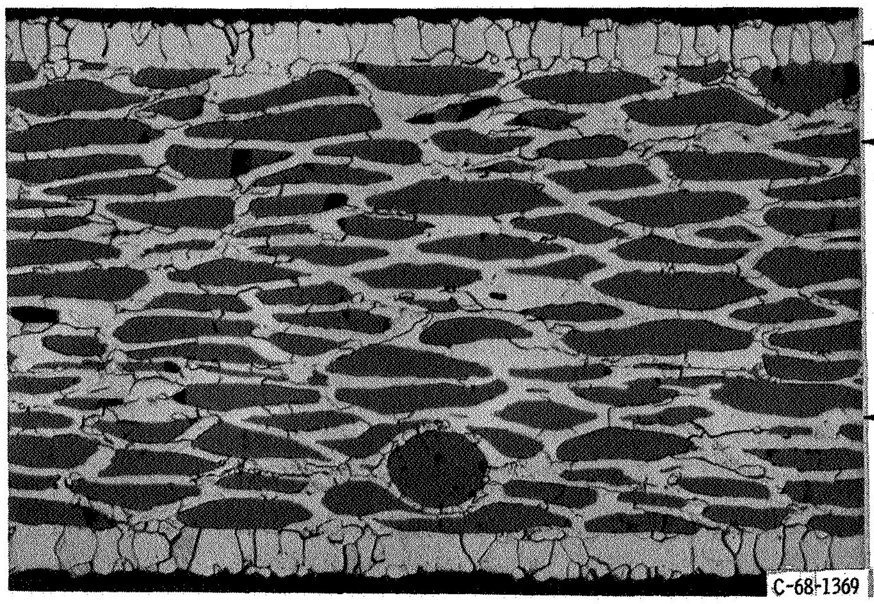

Figure 2. - Typical microstructure of specimens tested; tungsten-50-volume percent uranium dioxide cermet, with vapor deposited tungsten cladding. Etchant, Murakami's reagent. X150.

matrix. Although most of the UO_2 particles were deformed in the direction of rolling, a few randomly distributed particles showed little deformation. The reason for this nonuniform UO_2 deformation is unknown but it is suspected that locally high concentrations of impurities such as carbon may increase the hardness of the undeformed particles and increase their resistance to deformation. The presence of these few undeformed particles is believed to have little, if any, effect on the properties of the overall cermets.

Prior to testing, all specimens were heated in vacuum at 1950° C (3540° F) for at least 15 minutes to stabilize the microstructure. Tungsten wire gage marks were cemented to the specimens by use of a tungsten powder-glycerin slurry. Heating to test temperatures resulted in a sintering of the powder, which bonded the gage marks in place.

Test Apparatus and Procedure

The high-temperature creep rupture testing furnaces used in this study are shown in figure 3. These furnaces permitted testing in a vacuum of about 5×10^{-7} torr (7×10^{-5} N/m^2) following initial outgassing of test specimen and furnace. The furnaces utilize split-type tungsten mesh heating elements. Temperature was measured and controlled by means of a W-W26Re thermocouple in direct contact with the center of the specimen.

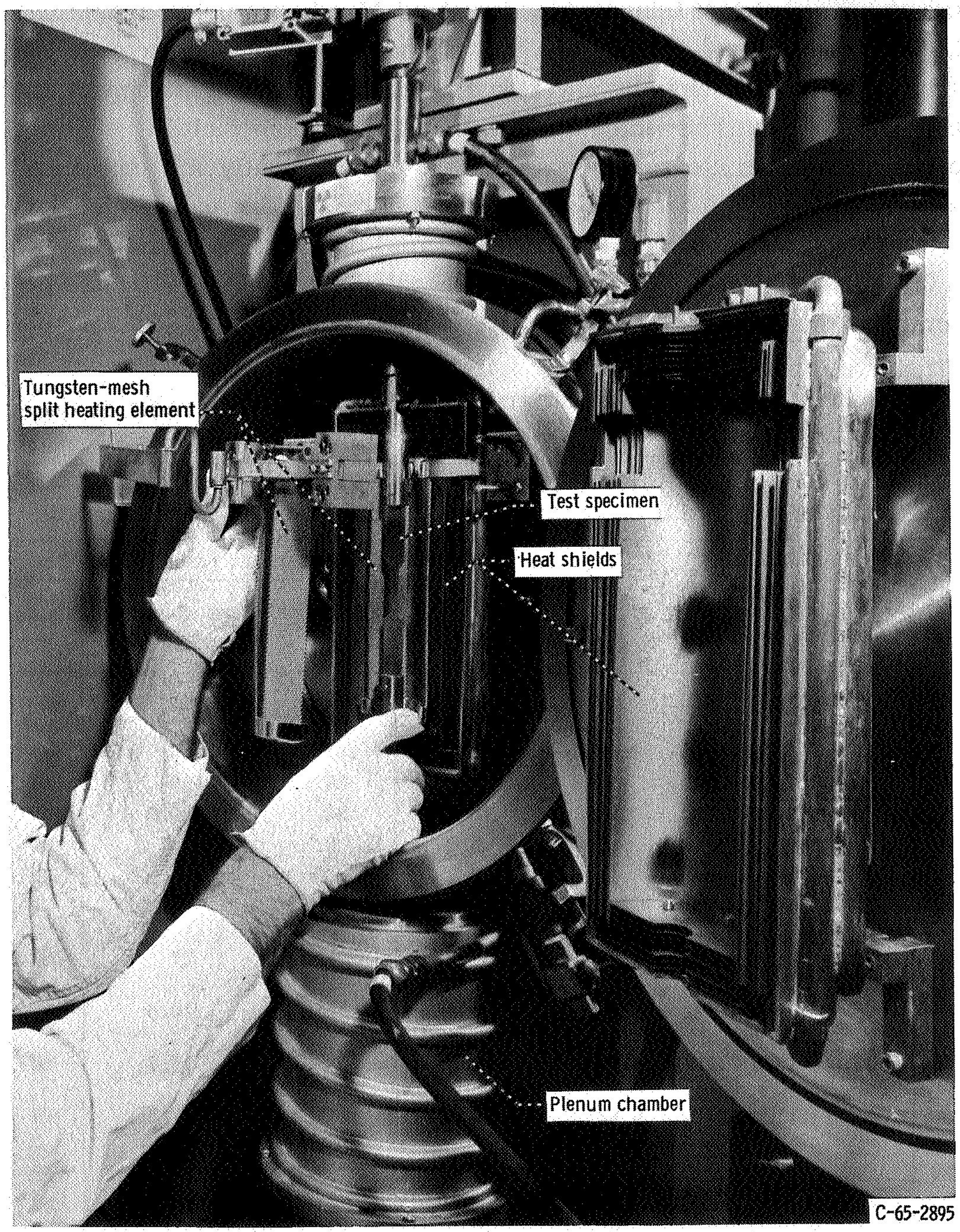

Figure 3. - High-temperature creep-rupture furnace.

The testing procedure followed in this program was to heat the test specimens at a rate at which a vacuum of at least 5×10^{-5} torr (7×10^{-3} N/m^2) could be maintained. The furnace was stabilized at test temperature for about 15 minutes prior to application of the dead load. During this time, initial gage length measurements were taken. The load was then applied to the specimen by lowering a hydraulic jack weight support at a rate of about 0.010 inch (0.25 mm) per minute. This eliminated the possibility of shock loading the specimen. Elongation measurements were taken periodically until specimen failure. These measurements were made with a cathetometer by sighting on gage marks applied to the specimen's gage section at a 1-inch (25.4-mm) interval. A measuring reproducibility of 0.0002 inch (0.005 mm), inclusive of operator error, was estimated for use of this instrument at this gage length.

TABLE II. - CREEP AND RUPTURE DATA FOR TUNGSTEN-CLAD, TUNGSTEN-50-VOLUME-PERCENT URANIUM DIOXIDE CERMET MATERIAL

Stress		Test temperature		Minimum creep rate, %/hr	Time, hr, to reach -			
psi	MN/m^2	^{o}C	^{o}F		0.5 percent strain	1.0 percent strain	end-of-second stage creep	Rupture
1740	12	1650	3000	0.0095	39.2	91.6	133	696
5075	35	1370	2500	0.0048	100	185	83	(a)
		1427	2600	.0200	16.6	37.5	60	158
		1480	2700	.0263	19	38	40.5	140
		1540	2800	.090	4.6	9.3	6	26
		1650	3000	.11	3.3	6	2	19
		1800	3270	.75	1.2	1.7	1.2	4
8000	55	1350	2462	0.0308	12.6	29	27	59
10 500	72	1300	2372	0.048	10.6	22.6	20.6	39
12 380	85	1300	2372	0.041	7.9	8.5	19.7	44
13 850	95	1300	2372	0.085	2.3	7.5	7.5	19
14 500	100	1080	1975	0.002	150	390	320	618
		1093	2000	.00126	208	442	180	644
		1120	2050	.00435	61.6	177	177	359
		1160	2125	.0142	33.3	83.3	78	99
		1300	2372	.150	2.3	5.2	~3	10
		1450	2640	1.4	.3	.4	.3	1

[a]Test terminated at 1300 hr because of gradual temperature drop. Specimen appeared to be near end of rupture life.

The specimens were tested at temperatures of 1080° to 1800° C (1975° to 3272° F). Most of the tests were run at stresses of 5075 and 14 500 psi (35 and 100 MN/m^2, respectively); however, supplementary data were obtained at stresses as low as 1740 pounds per square inch (12 MN/m^2). A rupture life of 696 hours was the longest test life obtained during this study.

RESULTS AND DISCUSSION

Creep-Rupture Results

The rupture lives and creep data obtained in this study are summarized in table II. Typical creep curves are shown in figure 4, which includes the families of creep curves

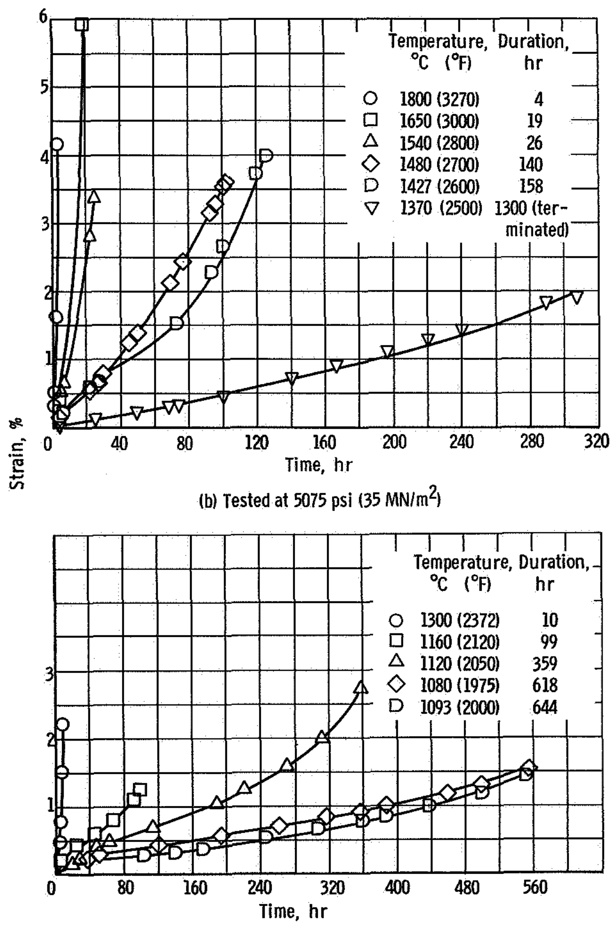

(b) Tested at 5075 psi (35 MN/m^2)

(b) Tested at 14 500 psi (100 MN/m^2)

Figure 4. - Creep curves for tungsten clad, tungsten-50-volume-percent uranium dioxide cermets.

based on isostatic stress data taken at 5075 and at 14 500 psi (35 and 100 MN/m^2, respectively). Time-temperature parameter calculations for obtaining various percentages of creep strain were calculated from these data, as were predictions of rupture strength.

All of these tests exhibited either three-stage or four-stage creep behavior, although the time scale used in figure 4 favors the longer term tests and obscures the intermediate stages of creep in the shorter term tests. The data in table II indicate that the end of the linear second stage creep occurs before or near the 1 percent creep strain level. (The values for the end of second stage creep were obtained from plots which used a larger scale than that of figure 4 so that the various stages of creep were more easily discernible.) The strain against time plots indicate that in some cases two linear creep rates (second and third stage) were observed. However, in these instances the rate of third stage creep always was greater than the rate of second stage creep. The second stage creep rate was considered to be the true creep rate, since it is the minimum rate and was observed in all cases. Therefore, this value was used in all tables, graphs, or calculations requiring creep rate data in this report.

Creep-Rupture Predictions

In order to derive the maximum benefit from the data obtained in this study, it is necessary to be able to interpolate and extrapolate beyond the actual test data points. Several time-temperature parameters have been devised for this purpose, the most widely known being the Manson-Haferd linear parameter, the Larson-Miller parameter, and the Dorn parameter. Although the applicability of these parametric prediction methods has not yet been fully evaluated for use with cermet materials, Conway's evaluation (ref. 4) of their use for refractory metals indicates that the Manson-Haferd parameter yields the most accurate predictions. Therefore, the Manson-Haferd parameter was used to extend the creep and rupture property values obtained in this study.

Using the Manson-Haferd parameter and the data previously presented in table II, longer term creep-rupture values were calculated for 0.5 percent creep, 1.0 percent creep, end of second stage creep, and rupture as described in appendix A. These predicted values are shown in figure 5 for temperatures of 1100°, 1300°, 1500°, and 1650° C (2012°, 2372°, 2732°, and 3000° F, respectively). This figure shows that in most cases the end of second stage creep lies between 0.5 and 1.0 percent creep strain, as was mentioned earlier. Thus, these plots emphasize that strain calculations used for conservative design purposes should be limited to low values (0.5 percent or less) of creep strain when coated particle, roll-compacted $W\text{-}UO_2$ cermets are being considered. This is particularly important at the lower temperatures (1100° and 1300° C; 2012°

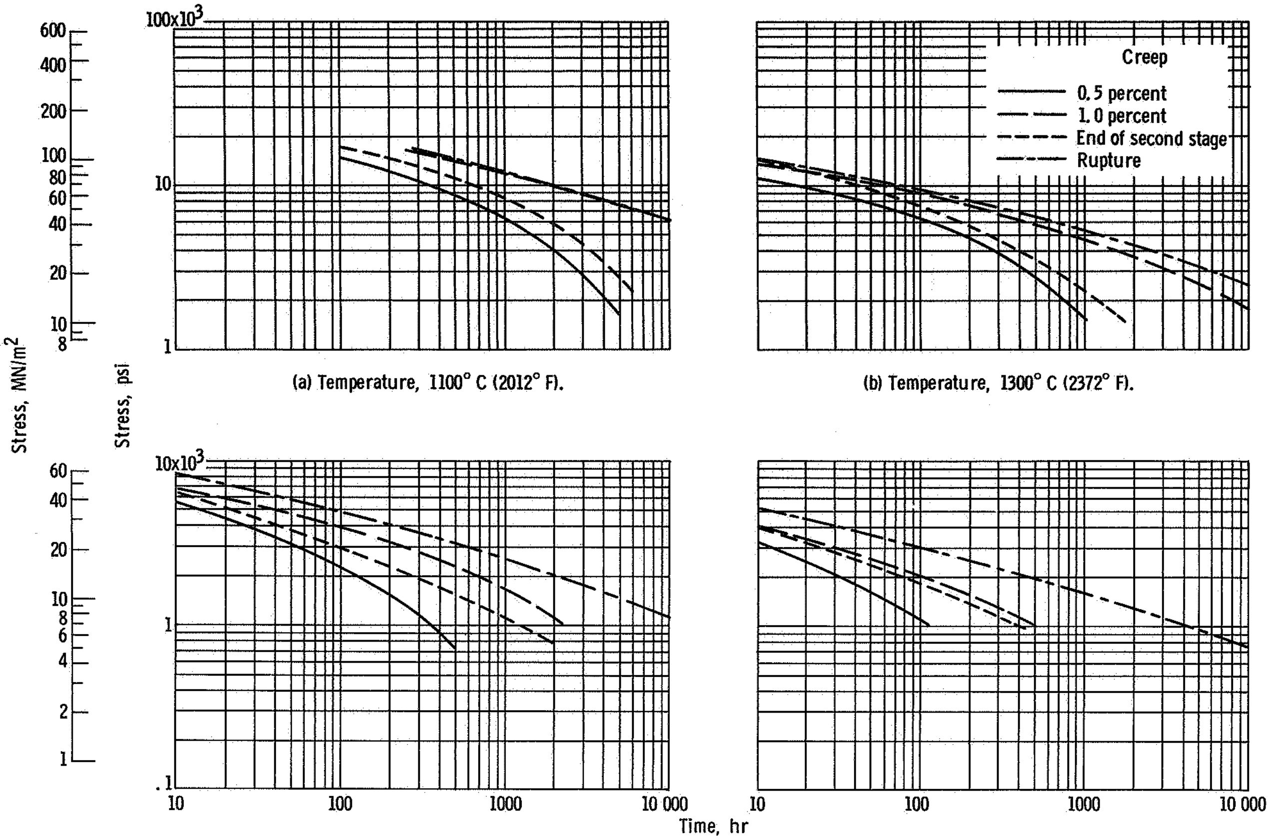

(a) Temperature, 1100° C (2012° F).

(b) Temperature, 1300° C (2372° F).

(c) Temperature, 1500° C (2732° F).

(d) Temperature, 1650° C (3000° F).

Figure 5. - Stress and time to reach 0.5-percent creep, 1.0-percent creep, end-of-second-stage creep, and rupture for tungsten-50-volume-percent-uranium dioxide cermets. (Plots derived by use of Manson-Haferd parameter.)

and 2372° F, respectively) where the times for 1.0 percent creep are very close to those for rupture.

Metallographic Examination

The photomicrographs of figure 6 show the types of fracture observed for the cermets tested near the highest and the lowest temperatures used in this study. The specimen tested at 1093° C (2000° F) (fig. 6(a)) had an initial stress of 14 500 psi (100 MN/m^2), while the specimen tested at 1650° C (3000° F) (fig. 6(b)) was stressed at 1740 psi (12 MN/m^2). The specimens had similar rupture lives of 644 and 696 hours, respectively.

In general, the fracture of the specimen tested at the lower temperature appears "clean " as opposed to the ragged fracture of the higher temperature specimen. The low temperature specimen's fracture was localized, but the fracture of the higher tem-

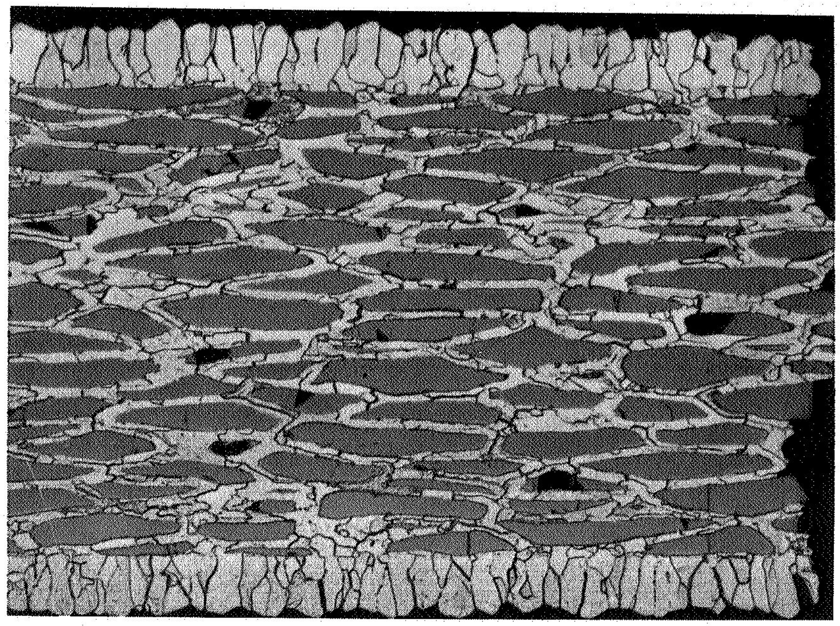

(a) Test conditions; temperature, 1093° C (2000° F); stress 14 500 psi (100 MN/m^2); rupture life, 644 hours.

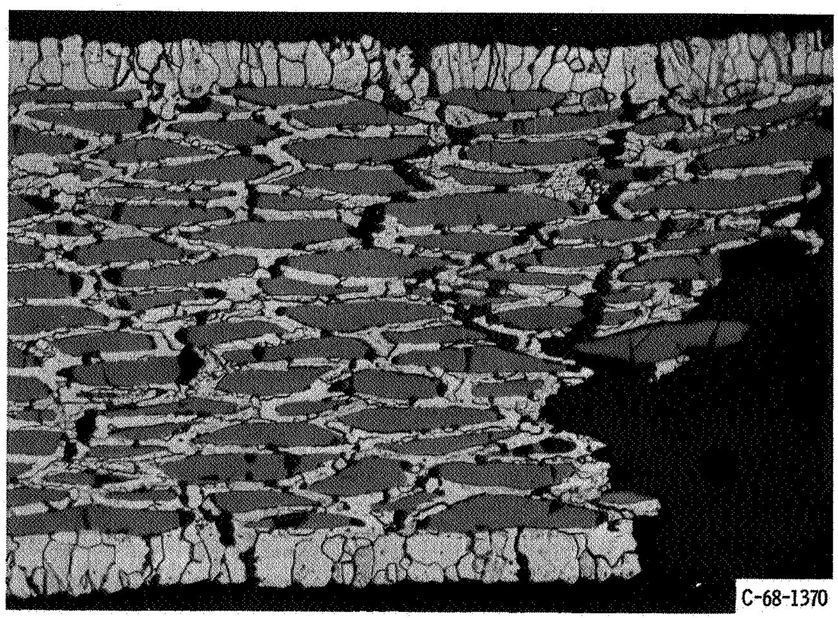

(b) Test conditions; temperature, 1650° C (3000° F); stress 1740 psi (12 MN/m^2); rupture life, 696 hours.

Figure 6. - Photomicrographs of roll-compacted tungsten-50-volume-percent uranium dioxide tungsten-clad cermets after creep-rupture tests. Murakami's etchant. X150.

perature specimen was distributed over a broad zone. Various factors contribute to the difference in appearance. The most obvious is the mode of fracture of the UO_2, which appears to fracture transgranularly at the lower temperature but appears to separate from the tungsten matrix at the higher temperature. Examination of the fracture of intermediate temperature test specimens run in this study place the transition temperature for this change in behavior of the UO_2 between 1160° and 1300° C (2125° and 2373° F). Since this agrees with the ductile to brittle transition temperature of 1250° C (2282° F) reported by Tottle (ref. 5) for UO_2 tested at slow strain rates in a vacuum, ductility changes in the UO_2 may be partially responsible for this behavior. However, it is more likely that this fracture mode results from the UO_2 having a greater shear strength than the tungsten-to-UO_2 bond strength at the higher temperatures, while the converse appears to be true at the lower temperatures.

Attempts to determine the mode of fracture of the matrix tungsten by metallographic examination were inconclusive because of the nature of the material involved in this study. For example, the presence of the UO_2 and the elongated shape of the tungsten grains somewhat obscure observation of the true nature of tungsten fracture. The tungsten grains are elongated in the direction of rolling during cermet fabrication, and the stringered shape of the UO_2 creates an elongated grain boundary at the W-UO_2 interface. Consequently, pull-out of the UO_2 at the fracture makes it difficult to distinguish between the appearance of either a ductile transgranular fracture or an intergranular fracture. This is particularly true for specimens tested at lower temperatures (such as that shown in fig. 6(a)).

Although test temperature and strain rate affect the nature of the fracture in tungsten, as shown by Sikora and Hall (ref. 6), the broad fracture-affected zone apparent in the higher temperature cermet specimens (such as shown in fig. 6(b)) is thought to result from a different effect. This effect is the formation of small bubbles, or voids, at the grain boundaries of the matrix tungsten. Such bubbles have been observed by McCoy and Stiegler (ref. 7) to form in vapor deposited tungsten at high temperatures. These bubbles can coalesce and grow when the specimens are stressed and this can either weaken the material or affect the reproducibility of the test data. In this study, grain boundary bubbles were observed metallographically in the matrix of all cermets tested above about 1400° C (2552° F), and they may account in part for the data scatter observed at these temperatures (appendix A). An example of such bubble formation in the gage section of a tested cermet is shown in figure 7. The photomicrograph was taken at about 1/4 inch (6.3 mm) away from the actual fracture. The cause of these bubbles is not fully understood, but they are thought to result from grain boundary impurities vaporizing at high temperatures. Fluorides are the impurities most highly suspected. Although the chemical analysis of these cermets indicated extremely low fluorine contents (<5 ppm, table I), it is conceivable that much higher concentrations could have been present in localized areas.

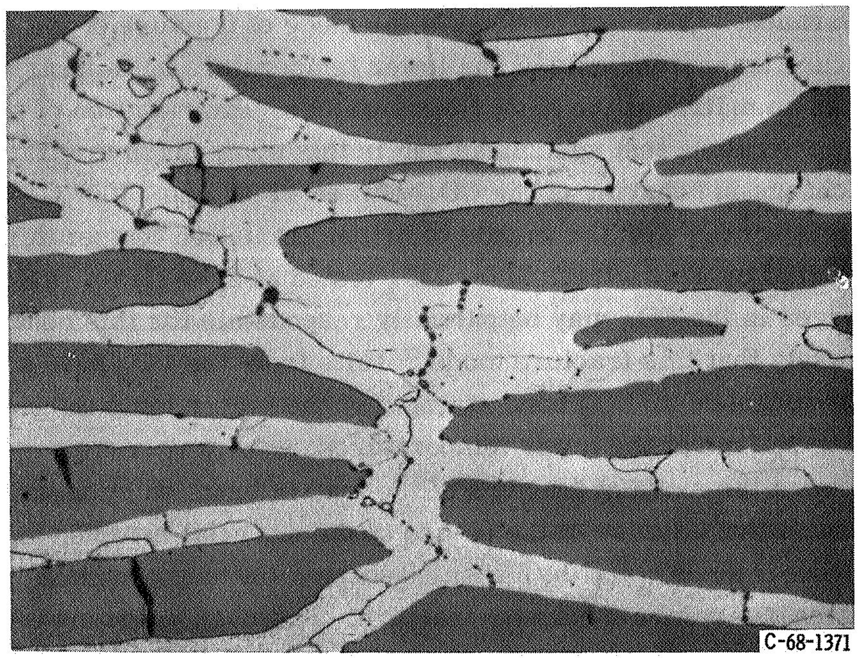

Figure 7. - Examples of grain boundary voids in tungsten-50-volume-percent uranium dioxide tungsten-clad cermets strained at high temperatures. Test conditions; temperature, 1650° C (3000° F); stress 5075 psi (35 MN/m^2); rupture life, 19 hours. Muramaki's etchant, X500.

The grain boundary voids probably serve as sites for the start of intergranular microcracks; however, the UO_2 particles in the cermets appear to serve as crack arrestors. This results in numerous localized microcracks in the cermets (as shown in fig. 6(b)). Thus, complete fracture of the specimen does not occur until a chain of these localized microcracks is formed across the entire specimen thickness. The additional time required for the cracks to connect results in larger total elongations and higher apparent strain capabilities. For example, the specimen shown in figure 6(b) (tested at 1650° C (3000° F)) exhibited a total elongation of about 11 percent compared to about 4 percent maximum for the specimens tested at lower temperatures. However, this higher apparent strain capability results from material failure and should not be considered as true ductility. Thus, methods of preventing such void formation need to be developed.

Activation Energy for Creep

The activation energy for creep of a metal may be used to gain some insight into the metal's mechanism of creep. Therefore, the apparent activation energy for creep was determined for the cermets evaluated in this study. Calculations for this determination are shown in appendix B. A stress dependency of the creep activation energy was found for this cermet. For example, at a stress of 5075 psi (35 MN/m^2), the apparent activation energy was 69 kilocalories per gram mole; at 14 500 psi (100 MN/m^2), it was 87.5 kilocalories per gram mole. The average value of 78 kilocalories per gram mole is in reasonable agreement with that of 74 kilocalories per gram mole reported for tungsten at 1650° to 1927° C (3000° to 3500° F) by Klopp and Raffo in reference 8 and suggests that the creep rate of the cermet material may be a function of the matrix tungsten alone.

Comparison with Unfueled Tungsten

To help evaluate the strength capabilities of the roll-compacted W-UO_2 cermet, its predicted rupture strength values were compared to literature values for unfueled tungsten. The 1650° C (3000° F) stress-rupture life isotherm for the W-UO_2 cermet is shown in figure 8, along with literature values for vapor deposited tungsten (ref. 7).

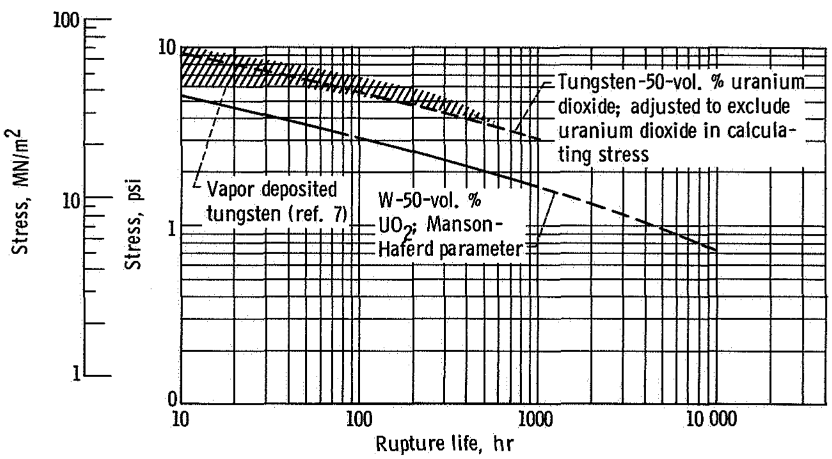

Figure 8. - Comparison of 1650° C (3000° F) stress-rupture lives for tungsten- and tungsten-clad tungsten-50-volume-percent uranium dioxide (W-50-vol. %-UO_2).

The 1650° C (3000° F) isotherm for vapor deposited tungsten was compared with that for the cermet since the matrix and cladding tungsten of the cermet were made from vapor deposited tungsten. The isotherm for the tungsten is shown as a scatter-band because various lots of this material yielded different results. In all cases, however, this material had a greater rupture life than that of the cermet material by a factor of about 10.

If the two materials are compared on the basis of stress required to attain a given rupture life, it appears that the vapor deposited tungsten can stand a stress of about 1.75 times that imposed on the cermet material. This factor of 1.75 is also the ratio of the tungsten (including cladding) to the UO_2 in a given cross sectional area of the cermet specimens. Therefore, by basing the stress imposed on the cermet during testing on the cross-sectional area of the tungsten alone, the two isotherms are comparable. This comparison is shown as a dotted line in figure 8. This comparison suggests that the rupture life of the cermet material may be controlled by the rupture life of the tungsten alone, and that the UO_2 particles merely lower the strength of the cermet below that of tungsten by effectively reducing the cross-sectional area of the load-bearing tungsten. The lack of a strength contribution by the dispersed oxide phase is probably due to its large particle size and poor bonding to the tungsten matrix.

A more valid indication of the role of the UO_2 in affecting the creep rupture properties of the cermet would be a comparison of the actual creep curves for the cermet and for unfueled tungsten. Since no appropriate data were found in the literature, a true comparison of this type could not be made. However, the cermet material in general appears more brittle than unfueled powder metallurgy or arc melted tungsten, as evidenced by the comparison of creep rate against rupture life for these materials described in appendix C. In addition, the 1650° C (3000° F) values of creep rate against rupture life for vapor deposited tungsten presented by McCoy in reference 9 fell within or near the scatter band of the cermet data of this study. This close agreement in data suggests that the low ductility of the cermet material may be solely a function of the vapor deposited matrix tungsten, and that the UO_2 does not further embrittle the cermet.

Elongation at or near fracture of the cermets was also quite low, as shown in figure 4. The value of about 4 percent total elongation at 1650° C (3000° F) (fig. 4(a)) agrees with data reported by McCoy (ref. 9) for vapor deposited tungsten, and is only about 10 percent of that reported for powder metallurgy tungsten.

CONCLUSIONS

Tungsten - 50 volume percent uranium dioxide (W-50 v/o UO_2) cermets, prepared by roll compaction of tungsten-coated UO_2 particles and clad with vapor deposited tungsten, were creep-rupture tested at temperatures ranging from 1080° to 1800° C (1975° to 3272° F). Several conclusions were drawn regarding the creep-rupture behavior of this material.

1. Rupture lives of the W-UO_2 cermets tested in this study ranged from 1 hour at 1450° C (2640° F) to 618 hours at 1080° C (1975° F) for the 14 500 psi (100 MN/m^2)

stress level, and from 4 hours at 1800° C (3270° F) to 158 hours at 1427° C (2600° F) for the 5075 psi (35 MN/m^2) stress level.

2. The stress-rupture life and ductility of dense W-UO_2 cermets produced from coated particles appears to be controlled by the vapor deposited tungsten phase. The dispersed UO_2 particles do not contribute to the strength of this type of cermet, probably due to their very large size and poor bonding to the matrix.

3. The W-UO_2 cermets entered the final stage of creep, where strain increases quite rapidly with time, at low strain levels (between 0.5 and 1.0 percent). At temperatures near 1100° C, the material ruptures after only about 1.0 percent creep strain. Therefore, care must be taken to limit design criteria for this type of material to strain levels of 0.5 percent or less.

Lewis Research Center,
National Aeronautics and Space Administration,
Cleveland, Ohio, April 12, 1968,
120-27-04-60-22.

APPENDIX A

LONG TERM CREEP-RUPTURE PREDICTIONS

Time-temperature parameters are frequently used to extrapolate the creep-rupture properties of metals. The parametric approach offers the distinct advantage of allowing for the accurate prediction of creep-rupture properties at stress levels, temperatures, and times beyond those at which tests were actually run. Several parametric methods have been used for such interpolation and extrapolation; however, the linear parameter developed by Manson and Haferd (ref. 3) is perhaps the most accurate of these methods. Conway's comparisons of the various methods (ref. 4) show this to be the case for all-metal systems. Since such comparisons have not as yet been made for cermet systems, the use of the Manson-Haferd linear parameter for this study was based on its proven performance with all-metal systems. This appendix describes the use of the Manson-Haferd linear parameter as it is applied to the data of this report to obtain 0.5 percent and 1.0 percent creep isotherms, as well as isotherms representing end of second stage creep and rupture life.

The Manson-Haferd linear parameter (P) may be expressed by the equation

$$P = \frac{T - T_a}{\log t_r - \log t_a}$$

where T is temperature, t_r is time to rupture, and T_a and $\log t_a$ are material constants.

This linear parameter is obtained by first plotting the logarithm of rupture life, $\log t_r$, against test temperature, T, using isostatic test data at two stresses. A straight line, usually obtained by the least squares method, is then fitted through each set of data points. The coordinates of the point at which these lines converge represent the material constants T_a and $\log t_a$. Knowing these values, a master curve which relates P to stress can be obtained by substituting experimentally-obtained time and temperature values into the linear parameter equation to calculate P. Once the master curve has been established for a given material, one may obtain rupture life data or isothermal plots by locating the P value which corresponds to the desired stress level and by again applying the equation to calculate "t_r" for the desired temperature. Extrapolation of the master curve beyond the range of the experimentally-obtained data points is not recommended, as in some cases the curve of the master plot may change. Also, extrapolation of predicted rupture life values beyond two time cycles (i.e., 10 000 hr predictions based on 100 hr data) has not yet been verified.

In this study, a plot of log t_r (in hours) against T (in ^{o}C) for W-50 v/o UO_2 isostatic stress data obtained at 5075 and 14 500 psi (35 and 100 MN/m^2) yielded material constants of log t_a = 7.55 and T_a = 500 (fig. 9). A master plot was then constructed (fig. 10) by using the linear parameter equation in conjunction with these data, and the curve was further defined by the use of supplementary data. Scatter in the test data is apparent in the figures, however, sufficient test specimens were not available to attempt to minimize the error by rerunning tests, nor to further extend the data by running longer time tests. The isotherms for various percentages of creep were also obtained by this method. Data used in all predictions are presented in table II of this report.

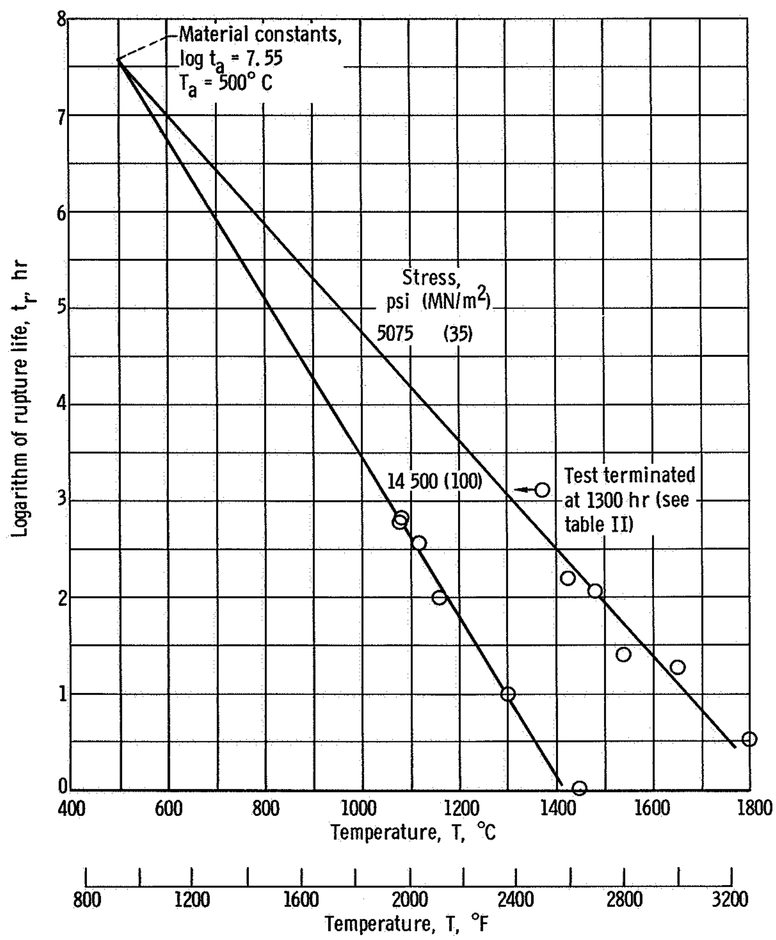

Figure 9. - Constant stress data for determination of Manson-Haferd linear parameter constants for tungsten clad, tungsten-50-volume-percent uranium dioxide cermet material. (See table II).

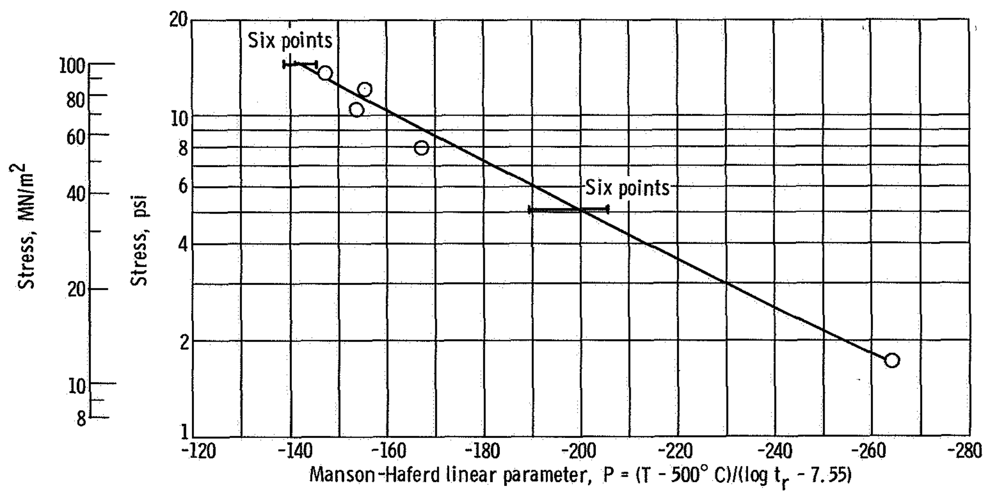

Figure 10. - Manson-Haferd linear parameter master plot for tungsten-50-volume-percent-uranium dioxide cermet material.

APPENDIX B

ACTIVATION ENERGY FOR CREEP

The activation energy for creep was obtained for W-50 v/o UO_2 cermets by use of the equation

$$\dot{\epsilon} = A e^{-Q/RT} \qquad \text{(ref. 10)}$$

where

$\dot{\epsilon}$ strain rate

R gas constant, 1.987 cal/(g mole)($^{\circ}$K)

T temperature, $^{\circ}$K

A constant

Q activation energy for creep, cal/g mole

Differentiation of this equation leads to the relation

$$\log_{10} \frac{\dot{\epsilon}_2}{\dot{\epsilon}_1} = \frac{Q}{2.3\,R}\left(\frac{1}{T_2} - \frac{1}{T_1}\right)$$

which is representative of an Arrhenius plot of the logarithm of the strain rate against 1/T, where $Q/2.3R$ is the slope of the line. A plot of the W-UO_2 cermet data at 5075 and 14 500 psi (35 and 100 MN/m^2) is shown in figure 11. A difference in the slopes of the two lines ($m = 1.5\times10^4$ and $m = 1.9\times10^4$, respectively) indicates that the activation energy is sensitive to stress. An average activation energy of 78 kilocalories (327 kJ) per gram mole was calculated from this plot.

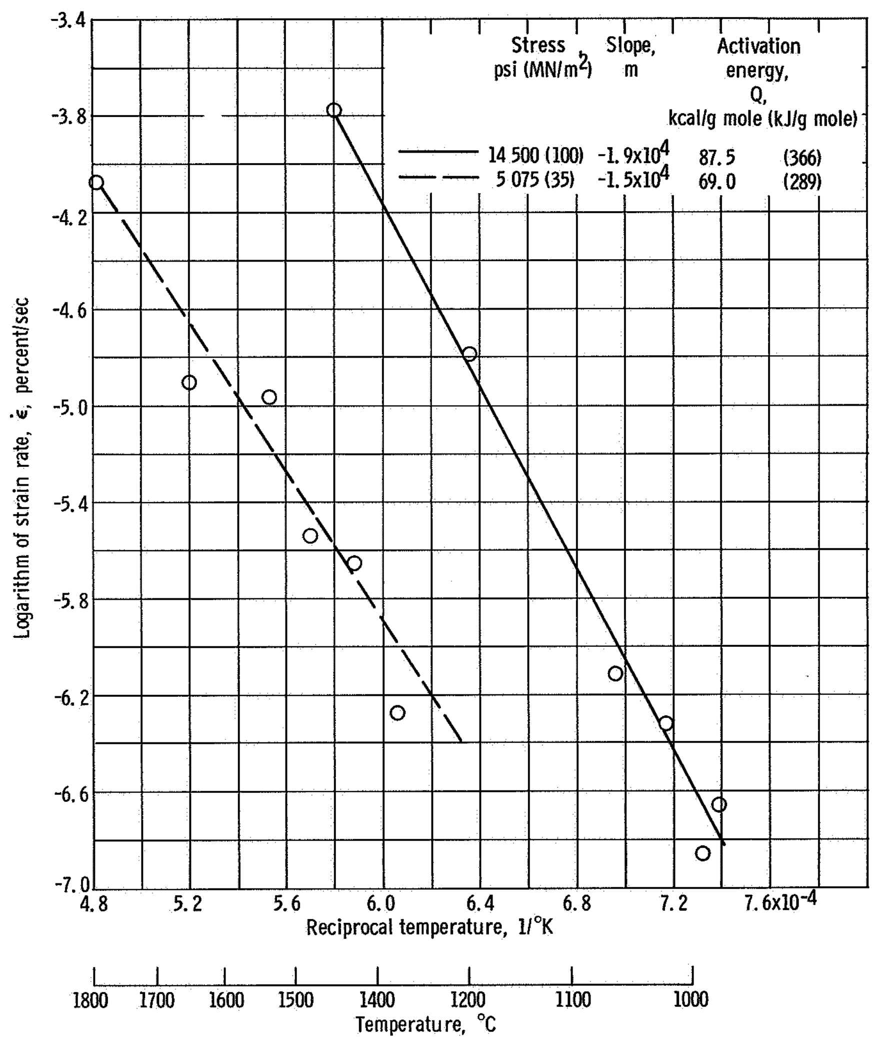

Figure 11. - Isostatic stress plot of tungsten-50-volume-percent-uranium dioxide cermet data for calculating activation energy for creep. Average activation energy, 78 kilocalories (327 kJ) per gram mole.

APPENDIX C

CORRELATION OF CREEP RATE AND RUPTURE LIFE

The method of correlating minimum creep rate and rupture life is based on the proposition that the product of steady-state creep rate and rupture life of annealed metals and single phase alloys is a constant independent of stress, temperature, and atomic number for a given type of structure. This relation may be written as

$$\log t_r + m \log \dot{\epsilon} = C$$

where

t_r rupture life

$\dot{\epsilon}$ steady-state creep rate

C a constant

m the negative slope of a plot of $\log t_r$ against $\log \dot{\epsilon}$

The relation has been shown to hold for several alloys (by Machlin in ref. 11 and by Monkman and Grant in ref. 12) and for unalloyed metals including tungsten (by Klopp and Raffo in ref. 8 and by McCoy in ref. 9).

Using the values obtained in this study, a plot of minimum creep rate against rupture life was developed for the roll-compacted W-UO_2 cermet. This is shown as least squares curve A in figure 12. The values of the constants derived from this plot are $m = 0.95$ and $C = 0.03$. The constant C is based on the shape of the creep curve, and can be used to relate the creep strain to a theoretical strain at rupture. This constant is directly proportional to the ductility (i.e., a low C value indicates a low ductility and vice versa).

Literature data show this method of prediction to be sensitive to materials variables, such as crystal structure and changes in ductility as a result of variations in testing temperature (ref. 12). For example, powder metallurgy tungsten tested at 1650° C (3000° F) by different investigators (plots B and C) yielded a variation in values of m and C, while arc-melted tungsten tested at this temperature (plot D) yielded a value of C quite close to one of the powder metallurgy values. The variation in powder metallurgy values is possibly due to a difference in material microstructures as a result of variations in fabrication history. The effect of changing ductility with testing temperature may be illustrated by the comparison of arc-melted tungsten tested at 1650° and

1930° C (3000° and 3500° F) (plots D and E) by Klopp and Raffo (ref. 8). The constant C changed slightly, the plot shifted to the left with increased temperature, and the slope m varied slightly from 1.1 at 1930° C (3500° F) to 1.2 at 1650° C (3000° F). A similar but reversed effect was also observed for the W-UO_2 cermets tested in this study, as is represented by the scatter band shown on either side of Plot A.

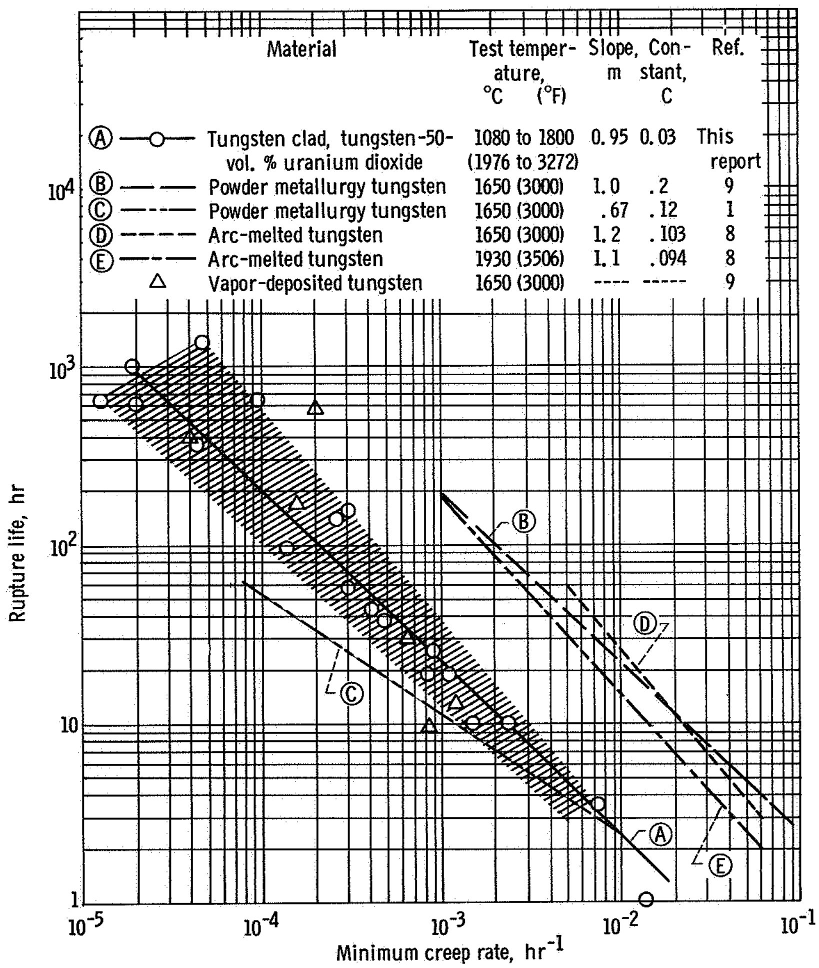

Figure 12. - Creep rate - rupture life correlation for tungsten and tungsten-clad tungsten-50-volume-percent-uranium dioxide.

REFERENCES

1. Buzzard, Robert J.: Factors Affecting High-Temperature Strength of Tungsten - Uranium Dioxide Composites. NASA TM X-1444, 1967.

2. Watson, Gordon K.; Caves, Robert M.; and Saunders, Neal T.: Preparation and Roll Compaction of Tungsten-Coated Uranium Dioxide Particles. NASA TM X-1448, 1967.

3. Manson, S. S.; and Haferd, A. M.: A Linear Time-Temperature Relation for Extrapolation of Creep and Stress-Rupture Data. NACA TN 2890, 1953.

4. Conway, J. B.: Properties of Some Refractory Metals. V. Numerical Methods for Creep and Rupture Analyses. Rep. GEMP-397, General Electric Co., Jan. 31, 1966.

5. Tottle, C. R.: Mechanical Properties of Uranium Compounds. Rep. ANL-7070, Argonne National Lab., Nov. 1965.

6. Sikora, Paul F.; and Hall, Robert W.: Effect of Strain Rate on Mechanical Properties of Wrought Sintered Tungsten at Temperatures Above 2500° F. NASA TN D-1094, 1961.

7. McCoy, H. E., Jr.; and Stiegler, J. O.: Mechanical Behavior of Chemically Vapor Deposited Tungsten at Elevated Temperatures. Rep. ORNL-4162, Oak Ridge National Lab., Sept. 1967.

8. Klopp, William D.; and Raffo, Peter L.: Effects of Purity and Structure on Recrystallization, Grain Growth, Ductility, Tensile, and Creep Properties of Arc-Melted Tungsten. NASA TN D-2503, 1964.

9. McCoy, H. E.: Creep-Rupture Properties of Tungsten and Tungsten-Base Alloys. Rep. ORNL-3992, Oak Ridge National Lab., Aug. 1966.

10. McLean, Donald: Mechanical Properties of Metals. John Wiley & Sons, Inc., 1962.

11. Machlin, E. S.: Creep-Rupture by Vacancy Condensation. Trans. AIME, vol. 206, no. 2, Feb. 1956, pp. 106-111.

12. Monkman, Forest C.; and Grant, Nicholas J.: An Empirical Relationship Between Rupture Life and Minimum Creep Rate in Creep-Rupture Tests. Proc. ASTM, vol. 56, 1956, pp. 593-605.